Supplementary Material

Carbon nitride assisted chemoselective C–H bond photo-oxidation of alkylphenoletoxylates in water medium

M. Ilkaeva,[a] I. Krivtsov,*[a,b] E. Bartashevich,[c] S.A. Khainakov,[d] J.R. García,[a] E. Díaz,[e] S. Ordóñez[e]

[a] *Departments of Organic and Inorganic Chemistry, Physical and Analytical Chemistry, University of Oviedo-CINN, 33006, Oviedo, Spain.*

[b] *Nanotechnology Education and Research Center, South Ural State University, 454080, Chelyabinsk, Russia.*

[c] *Department of Theoretical and Applied Chemistry, South Ural State University, 454080, Chelyabinsk, Russia.*

[d] *SCTs Facilities, University of Oviedo, 33006 Oviedo, Spain.*

[e] *Department of Chemical and Environmental Engineering, University of Oviedo, 33006 Oviedo, Spain.*

** Corresponding author, E-mail: UO247495@uniovi.es, Tel.: +34 985 103 030.*

1. Materials

Melamine, t-butyl alcohol, p-benzoquinone, p-cresol (all of 99 % purity), ethyl acetate (HPLC grade, 99.9 %), acetonitrile (HPLC grade, 99.9 %) and 30 wt % hydrogen peroxide were purchased from Aldrich. Hydrochloric acid 37-38 *wt* % water solution was obtained from J.T. Baker. Methanol, sodium hydroxide, potassium chloride were obtained from VWR Chemicals. For the photocatalytic test, 2-(4-methylphenoxy)ethanol (MPET), 4-(2-hydroxyethoxy)benzaldehyde (HEB) (both 98 %), 3-(2-methylphenoxy)ethanol (98 %), and 3-(2-hydroxyethoxy)benzaldehyde (95 %) were obtained from TCI Europe NV. 4-methylbenzyl alcohol, 2-(4-methylphenyl)ethanol, (4-methylphenoxy)acetic acid and 4-formylphenoxyacetic acid were purchased from Alfa Aesar.

2. Photocatalyst preparation

Bulk graphitic carbon nitride (g-C_3N_4) samples were prepared via the thermal condensation method from melamine following the procedure reported in ref. 1. 10 g of melamine was placed in a ceramic crucible covered with a lid and heated in a muffle furnace at 2 °C min^{-1} up to 520 °C, then left for 2 h at the reached temperature and slowly cooled down. The g-C_3N_4 sample derived from melamine was labelled as MCN. The bulk carbon nitride prepared from melamine (MCN) was used as the precursor for the thermally exfoliated g-C_3N_4[2]. For this purpose, 6 g of bulk carbon nitride was powdered in a mortar, evenly spread on the bottom of a ceramic bowl with a diameter of 14 cm, calcined in a static air atmosphere at 500 °C by using a temperature ramp of 2 °C min^{-1} and maintained for 4 h. The thermally exfoliated carbon nitride was coded as TE. MCN and TE samples were treated with hydrogen peroxide on the following way. To 1 g of MCN or TE samples 20 mL of H_2O_2 (30%) was added, then the suspension was mildly heated (70 °C) while stirring until the complete evaporation of the liquid, and finally, the solid samples were thoroughly washed with deionized water and dried at 70 °C in an oven. The H_2O_2-treated samples MCN and TE were designated as MCN_O and TE_O, respectively.

Also, the carbon nitride samples were treated with NaOH, HCl and KCl using the procedures reported in refs. 3, 4, and 5, respectively; they were designated as MCN_Na, MCN_W and MCN_K, respectively. For MCN_Na preparation,

1 g of MCN was placed in an autoclave and treated at autogenous pressure for 24 h at 180 °C; for MCN_W synthesis, 1 g of MCN was placed in 37% solution of HCl and stirred for 4 h; MCN_K was prepared by the thermal condensation of 10 g of melamine in presence of 7.5 g of KCl and 0.28 g of KOH at 520 °C for 2 h. All the samples were washed with distilled water and dried at 70 °C for 24 h before using applying them in the reactions.

3. Photocatalyst characterization

Powder XRD patterns were recorded in an X'pert PANanalytical diffractometer, using Ni-filtered Cu-Kα radiation source. Specific surface areas (SSA) were calculated in accordance with the standard Brunauer-Emmet-Teller (BET) method from the nitrogen adsorption data using a Micromeritics ASAP 2020. Infrared spectra of the samples were recorded with 4 cm^{-1} resolution using an ATR module of a Varian 620-IR spectrometer. Diffuse reflectance spectra (DRS) were obtained in air at room temperature in the 250–800 nm wavelengths range by means of a Shimadzu UV-2700 spectrophotometer, with $BaSO_4$ as the reference material. Mettler Toledo TGA/SDTA851 was used to investigate the thermal decomposition of g-C_3N_4 under an O_2 flow of 50 mL min^{-1} with the heating rate 10 °C min^{-1} in the temperature range 25–1000 °C. The binding energies of C, N and O and the surface elemental composition in the TE and TE_O samples were measured by X-ray photoelectron spectroscopy (XPS) by using a SPECS system equipped with a Hemispherical Phoibos analyzer operating in a constant pass energy, using MgKα radiation ($h\cdot\nu$ = 1253.6 eV). The solid state ^1H MAS NMR spectra were registered at spinning rate of 12 kHz using a Bruker Avance III 400WB spectrometer.

4. Photocatalysis procedure

The irradiation experiments were carried out in a Pyrex cylindrical photoreactor (internal diameter: 32 mm, height: 188 mm) containing 150 mL of aqueous suspension, irradiated by six external Actinic BL TL MINI 15 W/10 Philips fluorescent lamps emitting in the 340–420 wavelength range with the main emission peak at 365 nm. The reaction was carried out at about 25 °C and the reactor was provided by a thimble where water was allowed to circulate. Selected experiments were carried out in absence of O_2 by continuously bubbling N_2 throughout the runs to estimate the influence of O_2 on the reaction. The initial MPET concentration was 0.5 mM at the natural pH. The amount of a solid photocatalyst used for the experiments was 40 mg (80 mg for the recyclability study), except for the pristine carbon nitride MCN and MCN_O, for which 75 mg was used, due to their poorer light absorbance compared to the other samples. In this way, all the entering photons were virtually absorbed by the suspension. Some experiments were performed by reusing one of the best materials (TE_O) in order to verify its performance in a series of the consecutive reaction runs. Selected scavengers were used, in order to establish the reactive species responsible for MPET conversion and the selectivity to HEB. Methanol (MeOH) was used as a hole scavenger, t-butyl alcohol (t-BuOH) as an $^{\bullet}OH$ radical scavenger and p-benzoquinone to scavenge $^{\bullet}O_2^-$ radicals. The concentration of methanol, p-benzoquinone and tert-butyl alcohol scavengers was 2 mM. Samples of the irradiated solution were withdrawn at fixed time intervals. Then, the solution was filtered from the photocatalyst with 0.25 μm PTFE filter, extracted with ethyl acetate (at a volume ratio 1:1). Liquid aliquots were analyzed by a GC–MS technique, using a Shimadzu 2100 Ultra GC–MS equipped with a Teknokroma TRB-5MS (95%) dimethyl (5%) diphenyl polysiloxane copolymer column to identify and to determine the concentration of MPET, HEB and p-cresol. Standards purchased from Sigma-Aldrich and TCI with a purity >98% were used to identify the products formed during the reaction and to obtain the calibration curves. HPLC analysis of (4-methylphenoxy)acetic acid photo-oxidation products was carried out using

an Agilent 1200 Series instrument equipped with Agilent Eclipse CDB-C18 column. The determination was done in the flow of acetonitrile (20 %) and 13mM trifluoroacetic acid (80 %) at 40 °C

5. Calculations

Geometry optimization of dimelem, MPET molecules and theirs molecular complexes (Table S1) with and without hydrogen peroxide was carried out by Kohn-Sham method in B3LYP/6-311+G (d, p) approximation in the Firefly 8.0.1 program[6] with visualization in Chemcraft[7] package. The absence of imaginary vibration frequencies controlled in all cases. The resulting wave functions were used for QTAIM[8] analysis. The summarizing energy of interacted fragments was estimated with EML approach[9,10] as a sum of corresponding hydrogen bond energies between considered compounds in complexes. For that the potential energy density, $v(r_b)$, at the bond critical points r_b, of the electron density were calculated (see Table S1). The electron density (ED) and molecular electrostatic potential[11] (MEP) distributions were performed using Multiwfn[12] and MoleCoolQT[13] programs.

Table S1. Summarizing energy (kcal mol^{-1}) of HBs, the electron density (a.u.) and the potential energy density (a.u.) at the bond critical points in considerate complexes (see Fig. 4)

Dimelem – MPET	Dimelem – MPET		Dimelem – H_2O_2		MPET – H_2O_2	
dimelem–MPET (direct interactions)	-15.4		-		-	
HBs	$\rho(r_b)$	$v(r_b)$	-		-	
N…H-O	0.0329	-0.0254	-		-	
N-H…O	0.0172	-0.0112	-		-	
N-H…O	0.0146	-0.0092	-		-	
N…H-C	0.0067	-0.0033	-		-	
Dimelem–3H_2O_2–MPET	-8.6		-18.7		-20.7	
HBs	$\rho(r_b)$	$v(r_b)$	$\rho(r_b)$	$v(r_b)$	$\rho(r_b)$	$v(r_b)$
N…H-O	0.0326	-0.02429	-	-	-	-
N…H-C	0.0062	-0.00318	-	-	-	-
N…H-O	-	-	0.0246	-0.0169	-	-
N-H…O	-	-	0.0268	-0.0207	-	-
N-H…O	-	-	0.0289	-0.0220	-	-
O…H-O	-	-	-	-	0.0072	-0.0045
O…H-O	-	-	-	-	0.0435	-0.0401
O…H-C	-	-	-	-	0.0272	-0.0212

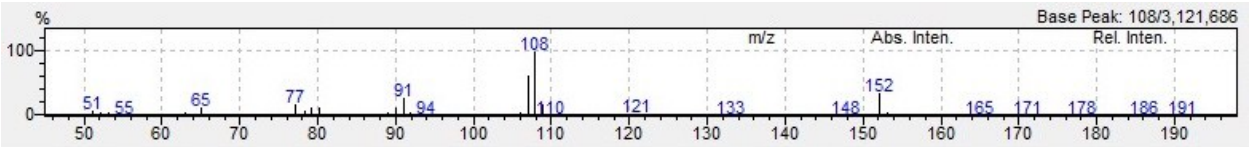

a

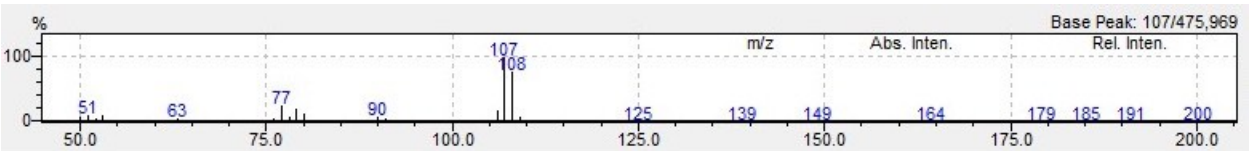

b

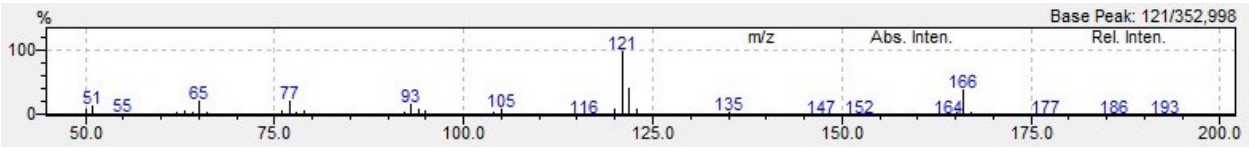

c

Fig. S1. Mass spectra for the MPET (a), p-cresol (b) and HEB (c) compounds.

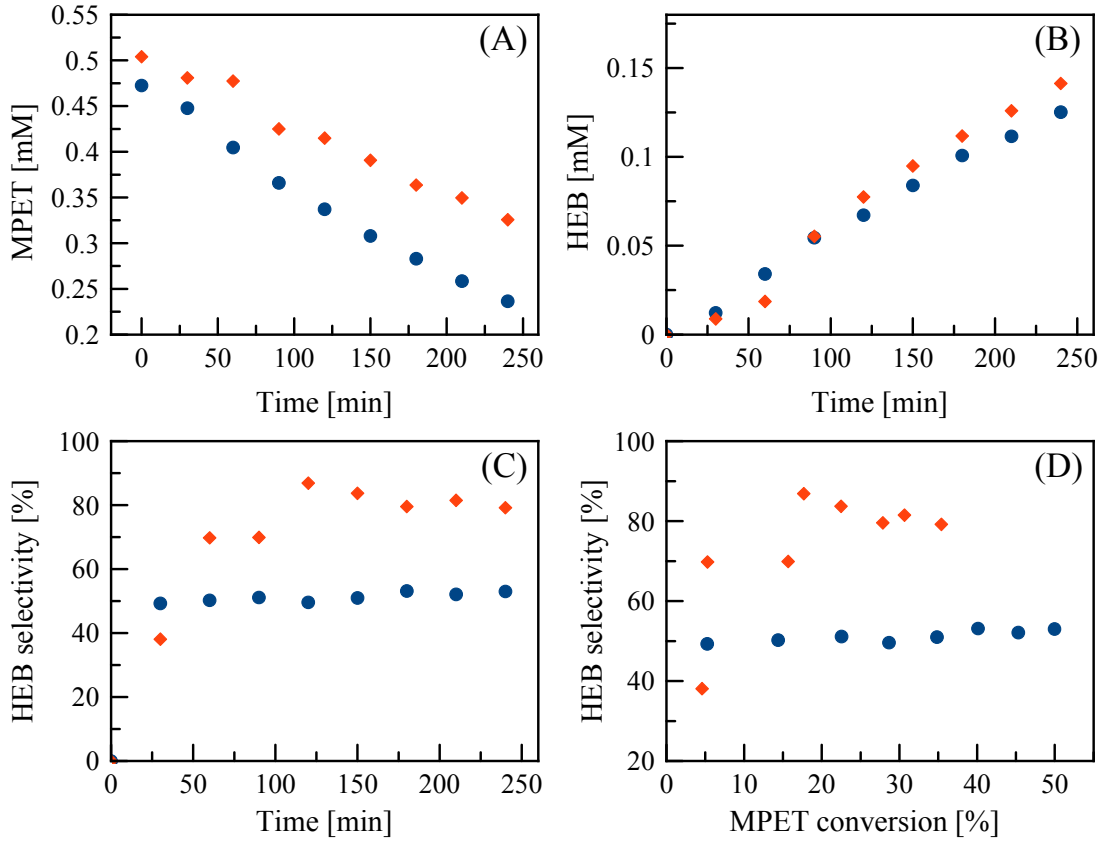

Fig. S2. MPET conversion (A); HEB formation (B); and selectivity to HEB versus irradiation time (C) or selectivity to HEB versus MPET conversion (D) in the presence of the non-exfoliated MCN (—) and H_2O_2-treated MCN_O (—).

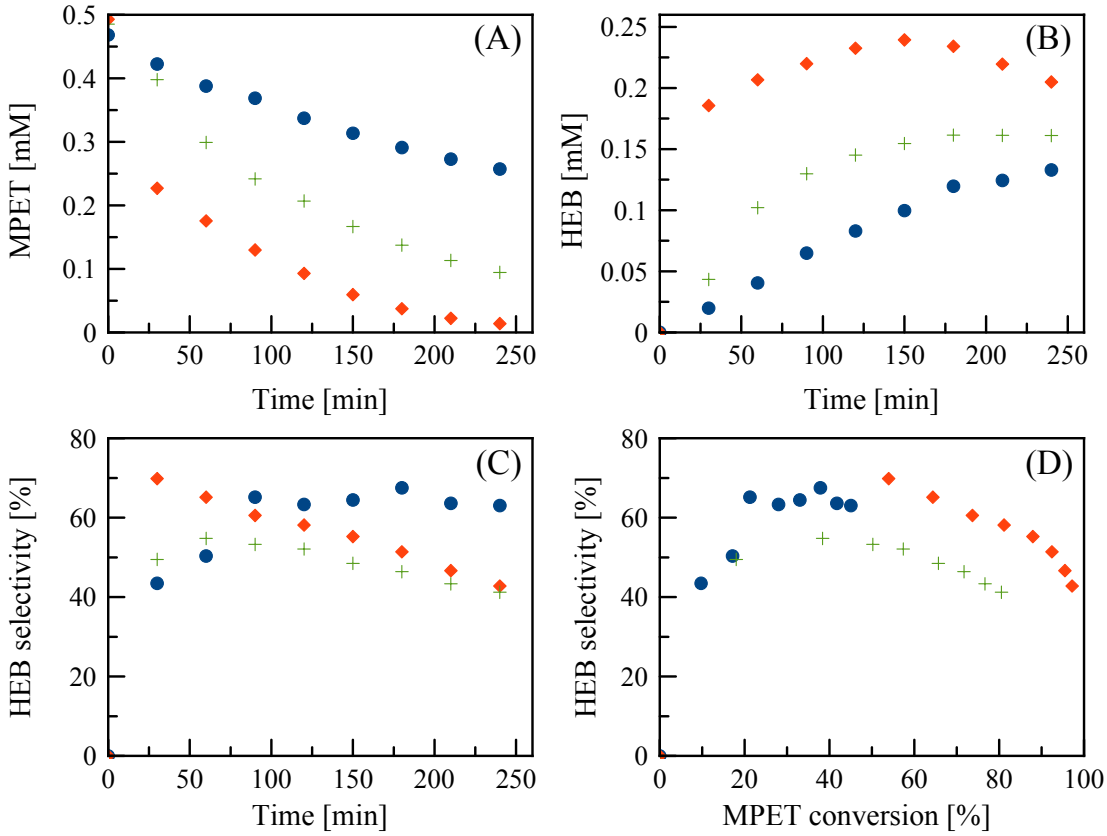

Fig. S3. MPET conversion (A); HEB formation (B); and selectivity to HEB versus irradiation time (C) or selectivity to HEB versus MPET conversion (D) in the presence of the MCN_K (—), MCN_W (—) and MCN_Na (—).

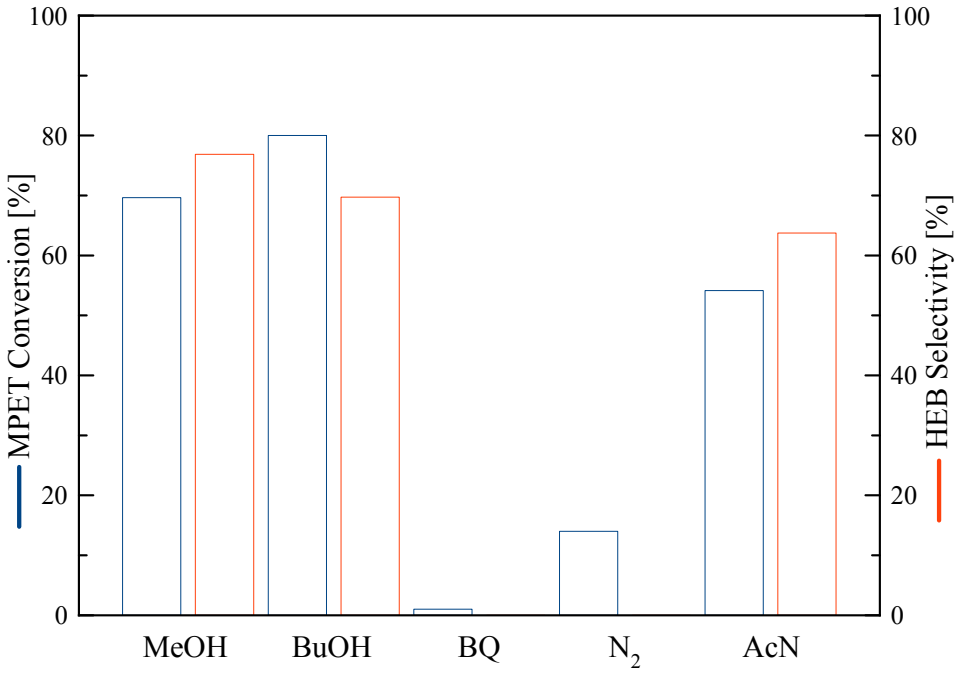

Fig. S4. Effect of using the scavengers (of charges and/or radicals) and acetonitrile (AcN) instead of water on the MPET conversion and the corresponding selectivity to HEB, after 240 min of irradiation in the presence of TE_O.

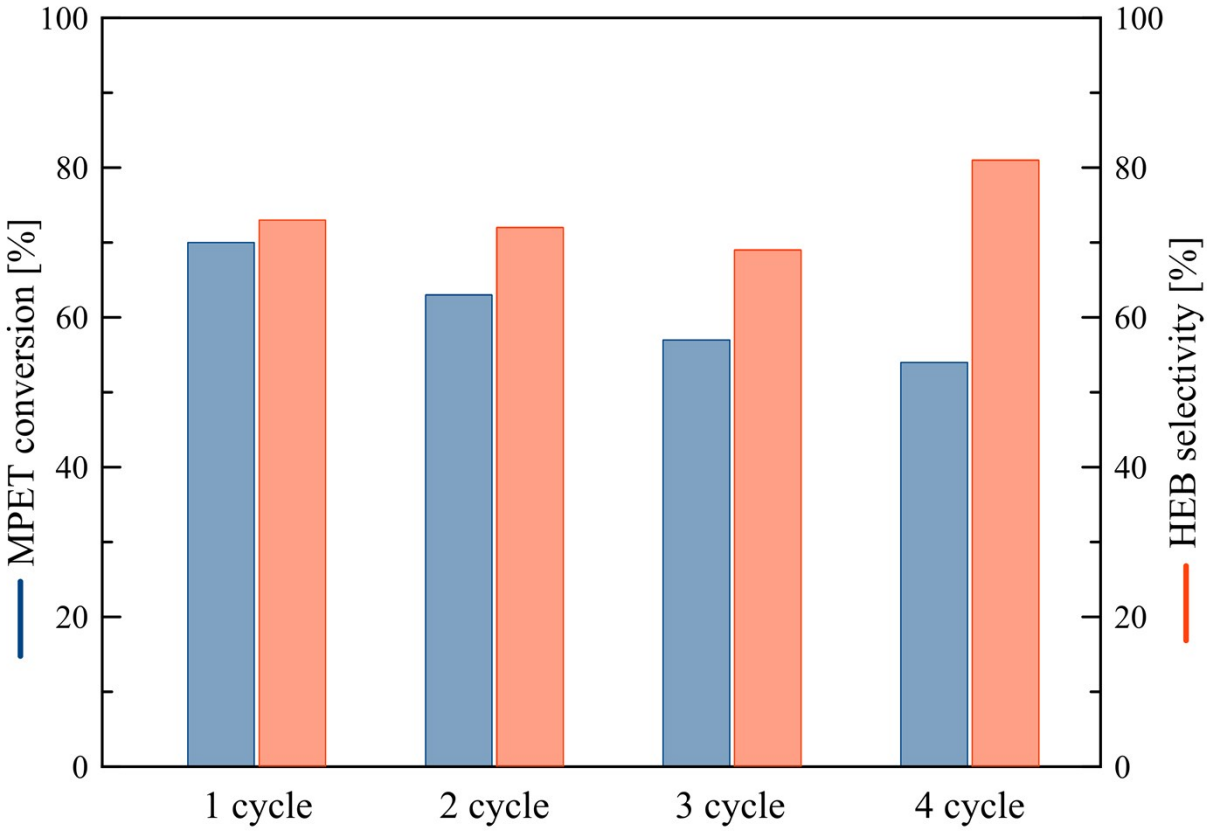

Fig. S5. The recyclability of TE_O in MPET conversion. The data is presented for 240 min of irradiation.

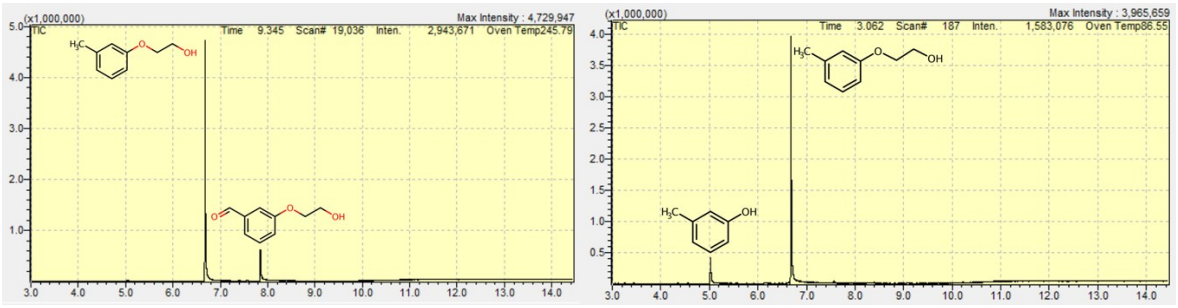

Fig. S6. To the left: Typical GC-MS data of the products of 3-(2-methylphenoxy)ethanol photo-oxidation in the presence of **TE** and **TE_O** photocatalysts after 4 h of irradiation. To the right: GC-MS data for 3-(2-methylphenoxy)ethanol photo-oxidation in the presence of **P25**

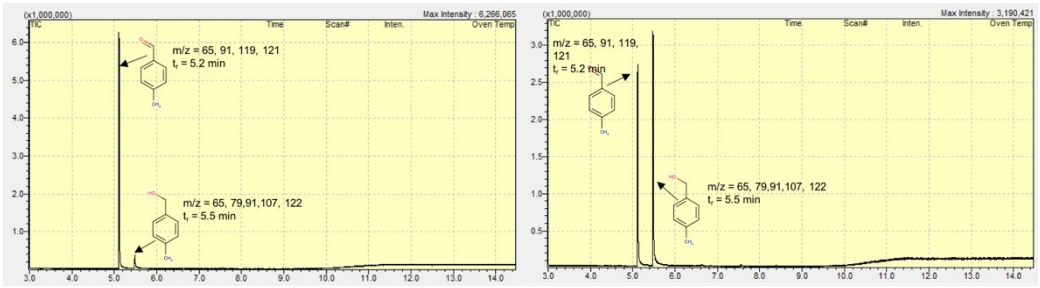

Fig. S7. GC-MS data of the products of 4-methylbenzyl alcohol photo-oxidation in the presence of **TE** (left) and **TE_O** (right) photocatalysts after 4 h of irradiation

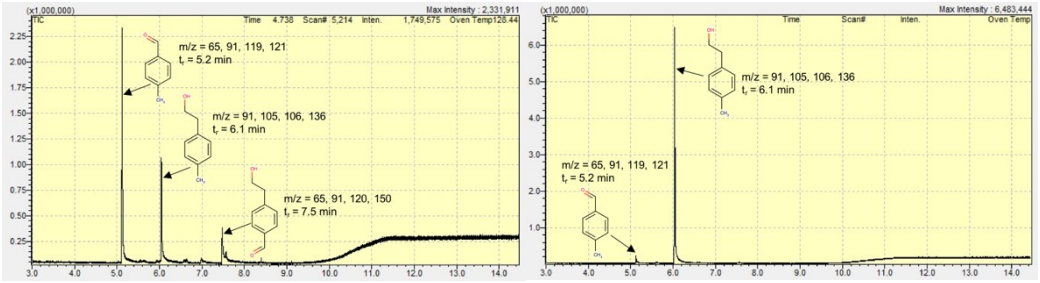

Fig. S8. GC-MS data of the products of 2-(4-methylphenyl)ethanol photo-oxidation in the presence of **TE** (left) and **TE_O** (right) photocatalysts after 4 h of irradiation

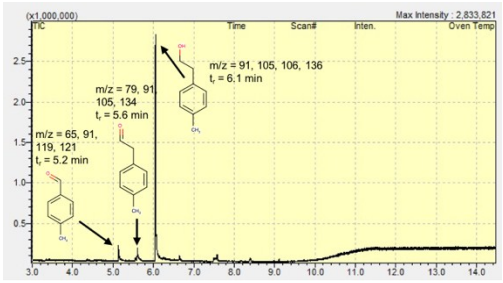

Fig. S9. GC-MS data of the products of 2-(4-methylphenyl)ethanol photo-oxidation in the presence of **P25 Aeroxide** photocatalyst after 4 h of irradiation

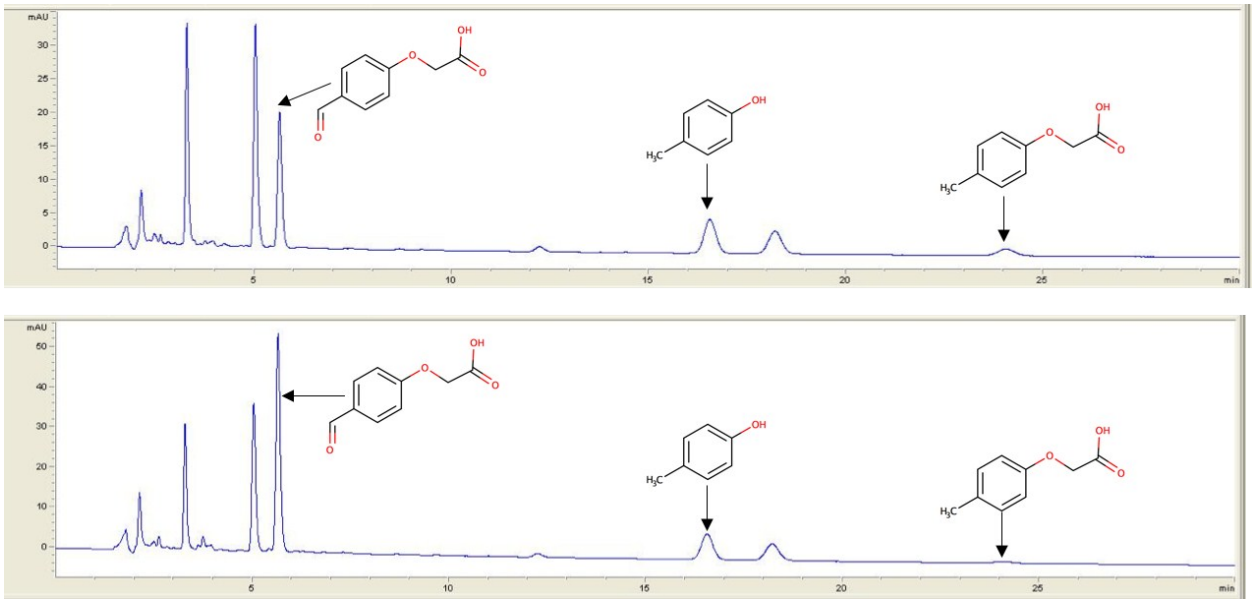

Fig. S10. HPLC chromatogram (230 nm) of products of (4-methylphenoxy)acetic acid oxidation in the presence of **TE** (top) and **TE_O** (bottom) photocatalysts after 4 h of irradiation

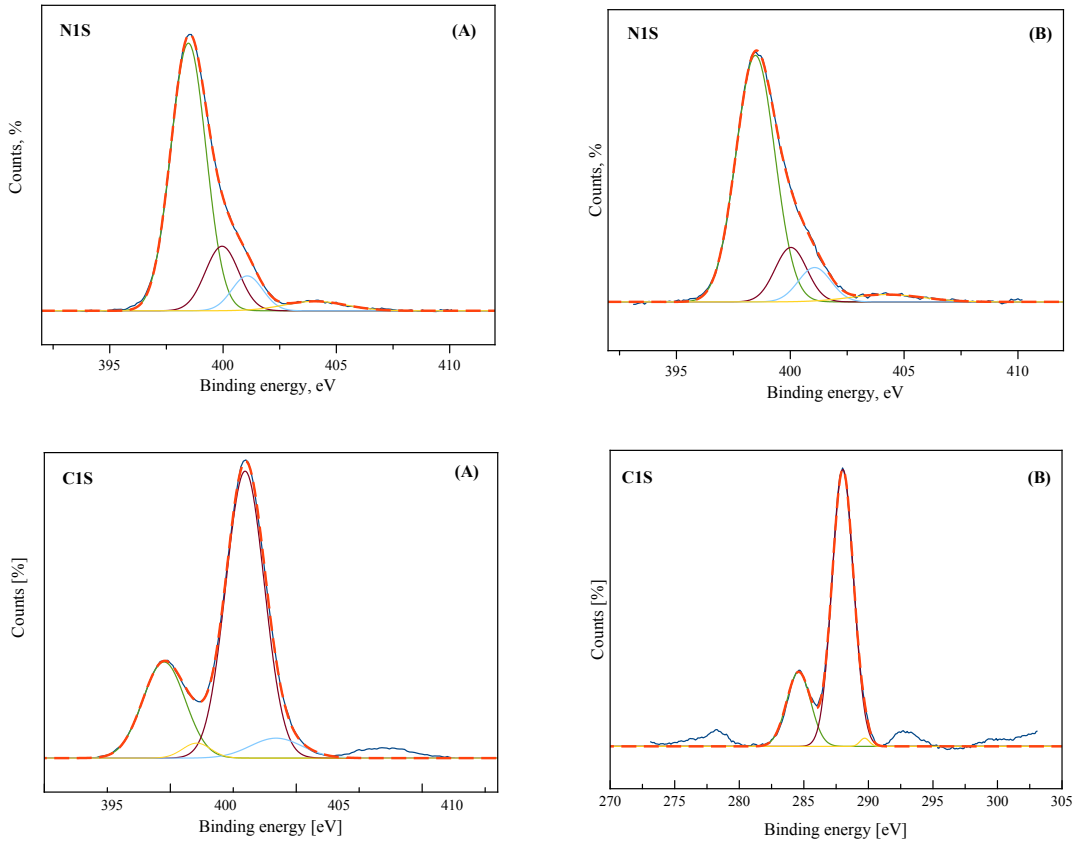

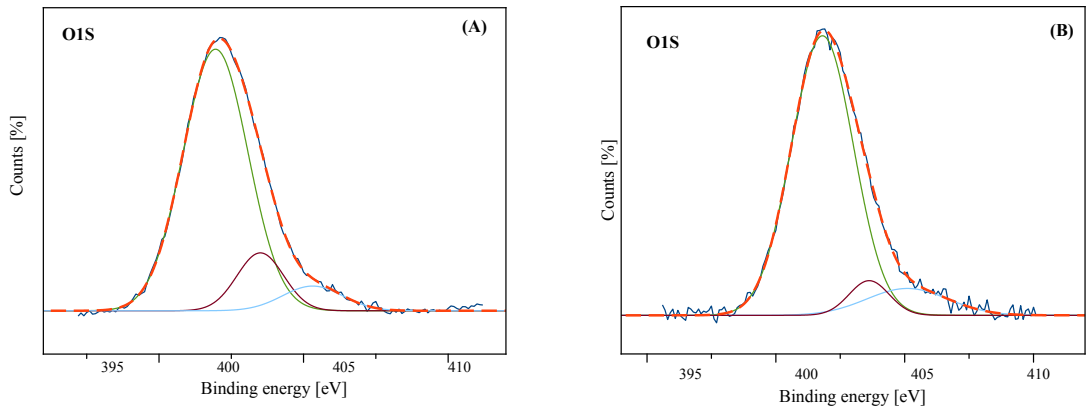

Fig. S11. XPS spectra of N 1s (A), C 1s (B) and O 1s (C) regions of the TE and TE_O samples.

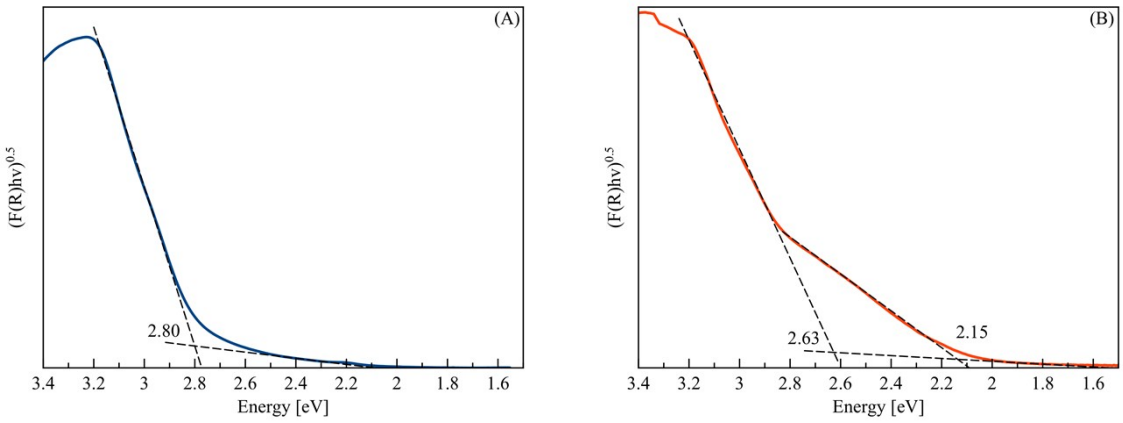

Fig. S12. Kubelka-Munk transformed DR UV-vis spectra of (A) TE and (B) TE_O samples.

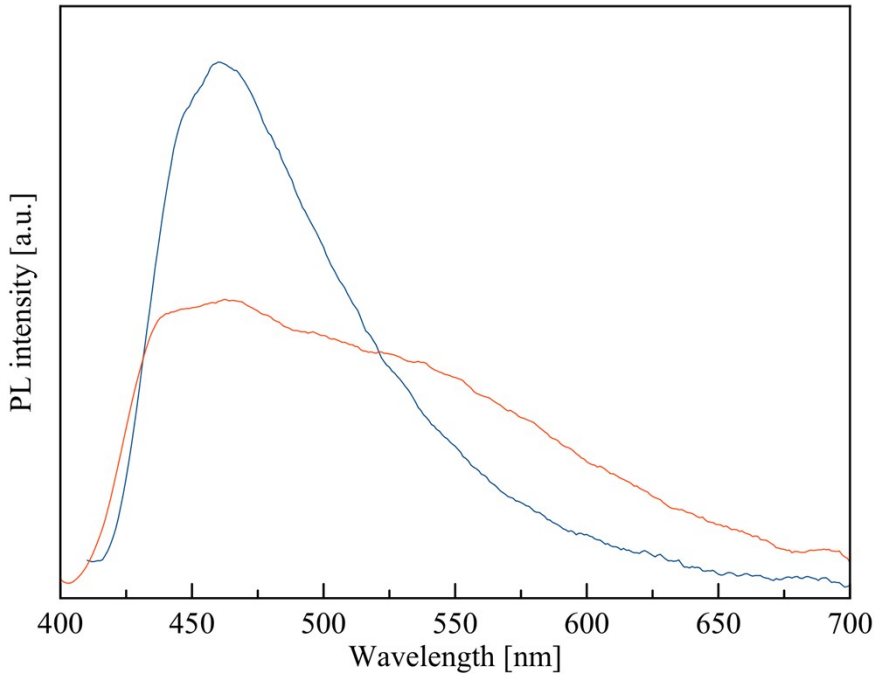

Fig. S13. PL spectra of (—) TE and (—) TE_O samples at 365 nm excitation.

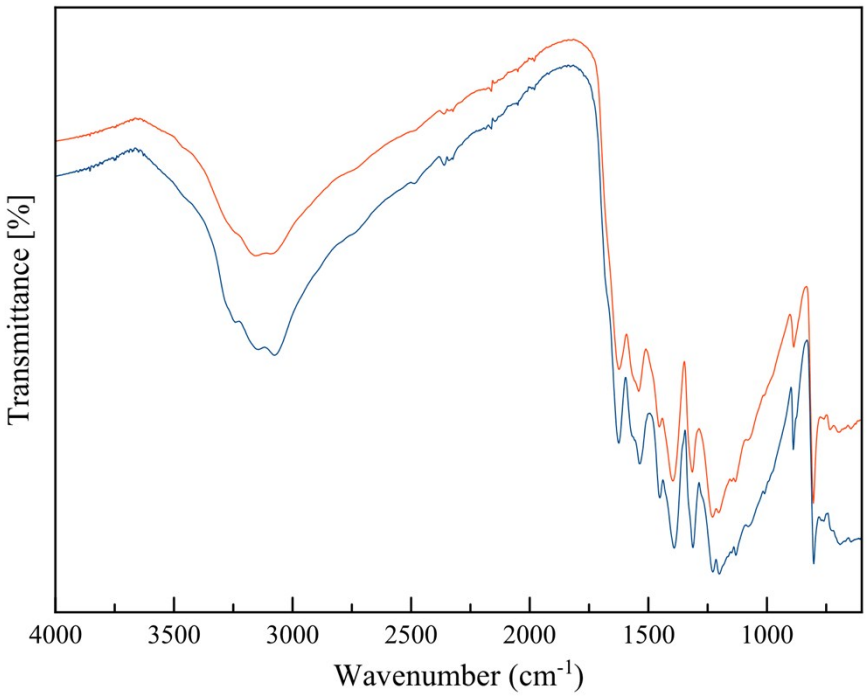

Fig. S14. FTIR of (—) TE and (—) TE_O samples.

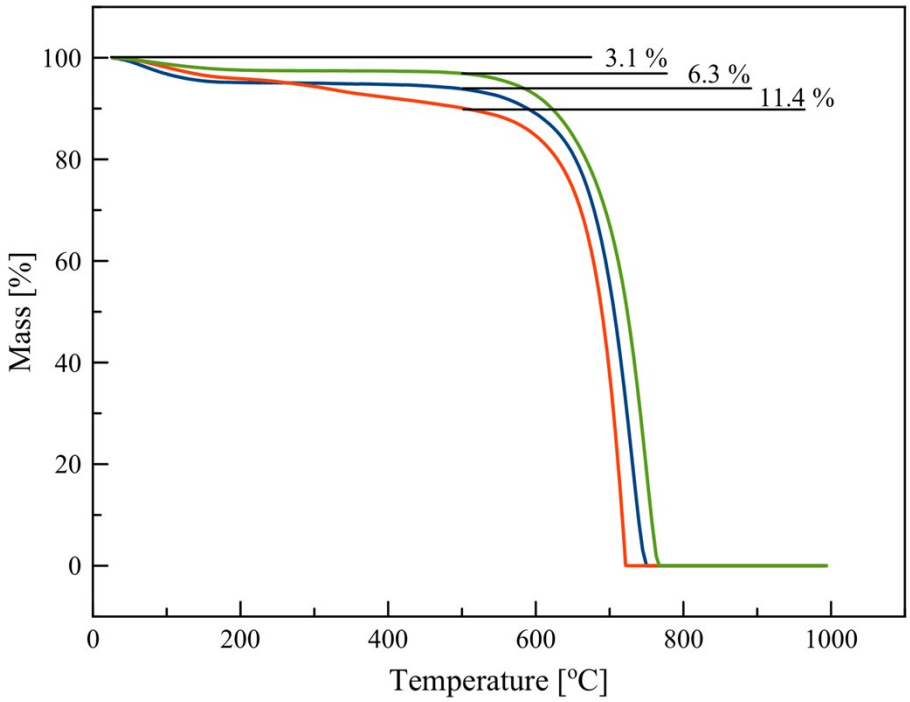

Fig. S15. Thermogravimetric study of (—) MCN, (—) TE, and (—) TE_O samples.

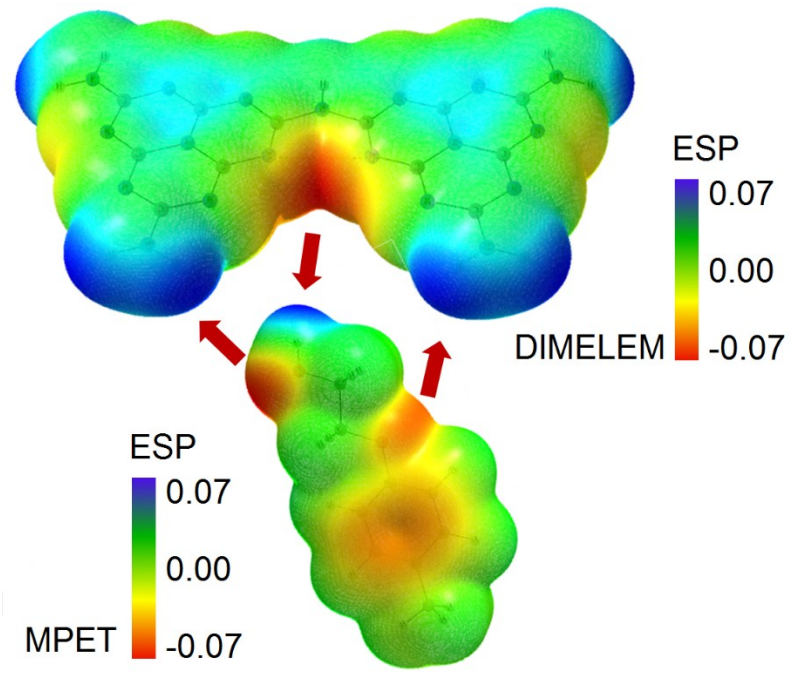

Fig. S16. Fragments complementarity of the dimelem and MPET that promotes to complex formation shown with molecular electrostatic potential (MEP) mapped on the isosurface of the electron density (ED) 0.001 a.u.

References

1. K. Wang, Q. Li, B. Liu, B. Cheng, W. Ho and J. Yu, *Appl. Catal. B*, 2015, **176–177**, 44.
2. **(a)** P. Niu, L. Zhang, G. Liu and H.M. Cheng, *Adv. Funct. Mater.*, 2012, **22**, 4763; **(b)** F. Dong, Y. Li, Z. Wang and W.K. Ho, *Appl. Surf. Sci.*, 2015, **358**, 393; **(c)** I. Krivtsov, E.I. García-López, G. Marcì, L. Palmisano, Z. Amghouz, J.R. García, S. Ordóñez and E. Díaz, *Appl. Catal., B*, 2017, **204**, 430.
3. T. Sano, S. Tsutsui, K. Koike, T. Hirakawa, Y. Teramoto, N. Negishi and K. Takeuchi, *J. Mater. Chem. A*, 2013, **1**, 6489.
4. Y. Zhang, A. Thomas, M. Antonietti and X. Wang, *J. Am. Chem. Soc.*, 2009, **131**, 50.
5. Y. Li, S. Ouyang, H. Xu, X. Wang,Y. Bi, Y. Zhang and J. Ye, *J. Am. Chem. Soc.*, 2016, **138**, 13289.
6. A. A. Granovsky. Firefly version 8. http://classic.chem.msu.su/gran/firefly/index.html
7. G. A. Andrienko, Chemcraft v.1.6, http://www.chemcraftprog.com/index.html
8. R.F.W. Bader, Atoms in Molecules. A Quantum Theory, Oxford University Press, New York, USA, 1990.
9. E. Espinosa, E. Molins, C. Lecomte, *Chem. Phys. Lett.* 1998, **285**, 170.
10. K.A. Lyssenko, A.A. Korlyukov, D.G. Golovanov, S.Yu. Ketkov, M.Yu. Antipin. *J. Phys. Chem.* 2006, A**110,** 6545.
11. Z. Shields, J.S. Murray, P. Politzer. *Int J Quant Chem*. 2010, **110**, 2823.
12. T. Lu, F. Chen, *J. Comput. Chem.* 2012, **33**, 580.
13. C. B. Hubschle and B. Dittrich, J. Appl. Crystallogr., 2011, **44**, 238.